Optimal Assignment of Time of Departure under Severe Weather [*]

Dabin Xue [1,2], Rui Sun [2,3], and Li-Ta Hsu[1**]

[1]Interdisciplinary Division of Aeronautical and Aviation Engineering,
Hong Kong Polytechnic University, Hong Kong
[2]Shandong Provincial Key Laboratory of Optical astronomy and Solar-Terrestrial Environment, China
[3]College of Civil Aviation, Nanjing University of Aeronautics and Astronautics, China

ABSTRACT

Severe weather poses a significant threat to flight safety and operation efficiency. A rerouting path is essential for aircraft to elude severe weather. Two issues related to rerouting are how to design a flight path and how to reduce operation time. We adopted ant colony optimization to design flight paths. The optimal time of departure was achieved through sensitivity analysis on various weights. Compared with current ground delay programs, the proposed solution can obtain the balance between total time and fuel consumption.

Keywords: Air Traffic Management，Fuel Consumption，Ant Colony Optimization，Time Cost， Real-time Reroute.

ACRONYMS

ATC:	Air Traffic Control
ATFM:	Air Traffic Flow Management
ACO:	Ant Colony Optimization
BADA:	Base of Aircraft Data
FAA:	Federal Aviation Administration
FPL:	Filed Flight Plan Message
FFA:	Flight Forbidden Area
GDP:	Ground Delay Programs
LP:	Linear Programming
NWS:	National Weather Service
TAS:	True Airspeed
WS:	Wind Speed

I. INTRODUCTION

The aviation industry has developed at an astounding pace over the past decades. Nevertheless, it is estimated that adverse weather results in about 70% delay events according to Federal Aviation Administration (FAA) statistics. Adverse weather, such as rain, fog, ice, snow, and dust, is a crucial factor for air traffic congestion. Under this situation, Air Traffic Flow Management (ATFM) plays an essential role. Traditional ATFM measures include Ground Delay Programs (GDP) and rerouting to avoid severe weather-affected regions. The former is an important strategy in ATFM and the purpose is to convert airborne delay into safer and more economic ground delay [1] with the sacrifice of the time cost. The latter is to achieve the minimum time cost and improve the airline operation efficiency but with the cost of fuel consumption because of a longer flight distance.

In recent years, this topic has attracted lots of attentions from researchers. Agustin et al [2] present a model to minimize objective functions, which allows for flight cancelation, total ground and air holding cost, delay cost for flights, penalty of alternative routes, etc. Bertsimas and Patterson [3] indicate that air traffic control (ATC) can adjust aircrafts' time of departure (ground-holding) or speed (airborne) in order to reduce the influence of traffic congestion in the air traffic system. Krozel et al [4] develop an objective function in order to balance the influence of weather-related delays and concerns for the workload of air traffic controllers or pilots.

Today, civil aviation faces two challenges: minimization of flight fuel consumption and minimization of elapsed flight time. To achieve these goals, Mirosavljevic et al show the impact of climb regime on flight profile of turbo-fan aircraft considering the usage of time, fuel and costs [5]. Liu et al build a real-time gate assignment model, and the delay costs of multi agent can be minimized simultaneously; the fuel consumption of each airline can be basically equalized by mixed set programming [6]. Turgut et al have indicated that each flight can save more than 40 kg fuel and 2 minutes time on average using continuous descent approach procedures instead of conventional procedures [7]. Wilson and Hafner have conducted three scenario simulations for the landings based on the airport of Atlanta and stated that the best saving conclusions on time, fuel consumption and distance they found are 45 hours, US$80,000 and 9,000 nautical miles per day [8]. Harada et al use dynamic programming for the trajectory optimization, and the research findings suggest that flight fuel consumption and flight distance can be saved by 312 kg and 19.7 km, respectively, on average for the object flights [9].

Any destructive weather phenomenon, which are hazardous to human life and property, is known as severe weather [10]. In order to ensure flight safety in severe weather, it is important to design a flight route for aircrafts to avoid the weather-affected zones. Wang et al [11] address the problem of determining a rerouting path, taking account of danger zones, flight segment length, turning angle and turning point number. Li et al [12] propose a new reroute planning method which is based on the multi-objective planning algorithm in terms of zonal severe weather areas. Bertsimas and Patterson [13] deal with the problem of searching for a path for aircrafts rerouting in terms of dynamically changing weather conditions in order to minimize delay costs.

Most of the aforementioned literatures on rerouting focus on the shortest path in stationary severe weather and conventional algorithms such as Dijkstra algorithm, Bellman-Ford algorithm. A* search algorithm have been made a further study [14], which can be used for the issue of mobile robot searching path to avoid obstacles. In paper [15, 16], grid-based search methods are applied to find a flight path around severe weather cells.

Researchers have developed many shortest path algorithms that are based on forecasted weather information in recent years. A rerouting algorithm has been investigated by Sridhar [17] in order to reroute around airspace whose capacities are exceeded. Prete [18] uses the A* algorithm to reduce the optimal routing problem by searching a graph for a shortest-path. Krozel [19] designs alternative paths for pre-departure flights around convective weather airspaces utilizing the latest weather forecast. However, none have made a study on the relationship between GDP and flight distance by dynamic rerouting. Conventionally, the time of departure is only decided by air traffic controllers, so airlines do not have flexible choices to decide the time to take off. However, as a result of detouring a severe weather area, an appropriately selected time of departure could significantly reduce the total cost, considering the relationship between fuel consumption and the total time including ground holding and travel time, as shown in our case study (see Figure 8). Moreover, the problems of finding the shortest flight path are solved separately and sequentially, the solutions would be suboptimal in practice, especially in dynamic weather conditions. In order to minimize flight distance, we have proposed a real-time rerouting algorithm. This paper makes contributions in the following three aspects:

(1) The optimization problem proposed in this paper seeks a balance between fuel consumption and total operation time including delay time and flight time by quantitatively analyzing their trade-offs. The optimization framework can be applied to scenarios with different priorities given to passengers and airlines.

(2) We use preceding radar image (Doppler weather radar mosaic) to demonstrate severe weather-affected region, because it is the foundation of real time rerouting. In this paper, we present a new model to define the flight forbidden area (FFA), and take pilots driving preference into consideration. Our filtering tool can be adjusted to filter different national weather service (NWS) levels to meet users' need of pilots and air traffic controllers.

(3) Ant colony optimization (ACO) is used to search for the shortest path for rerouting. A case study is conducted in order to avoid severe weather. Compared to stationary reroute, the results in dynamic reroute have shown a significant decrease in flight path length.

The rest of this paper is organized as follows. Section II introduces weather processing and equations of fuel consumption and flight time. Section III presents the multi-objective optimization. A case study of a flight path from Zhengzhou to Guangzhou is conducted in Section IV. Finally, Section V gives some concluding remarks.

II. WEATHER AND MODELS

A. Weather and Models

The input weather information, namely Doppler weather radar mosaic, shown in a two-dimensional form, is from China Central Meteorological Observatory (www.nmc.cn). The various vertically integrated liquid data, which are the integral of the reflectivity reading over a vertical column of airspace, are shown in different colors (see Figure 1 (*a*)). These data are divided into 7 weather levels (NWS Level from 0 to 6) according to measurements of radar reflectivity (in dBz), and they do have different effect on airplane operation safety (see Table 1 [4]).

As for the classification of FFA, researchers have defined FFA based on the severe weather forecast telegraph [20]. Li has proposed the method for establishing the static flight forbidden area using Graham algorithm and FFAs are divided into three categories, namely block FFA, zonal distribution FFA and scattered points distribution FFA in terms of the difference in the shape, influence scope, scale and distribution feature of FFA [21]. However, in the above two papers, the driving preference of pilots has not been taken into consideration. Rhoda et al [22] have indicated that pilots would choose to penetrate level 2 in en-route airspace, however, there are no chances that they would penetrate higher reflectivity. In our model, we do filtering on raw radar reflectivity data in order to eliminate the clusters of green weather cells (NWS Level 1 and 2). We retain the severe weather cells where NWS Level is 3, 4, 5 or 6(see Figure 1 (*b*)), namely FFA, because we use the weather avoidance algorithm, ant colony optimization, to avoid all such cells (NWS Level 3 or above).
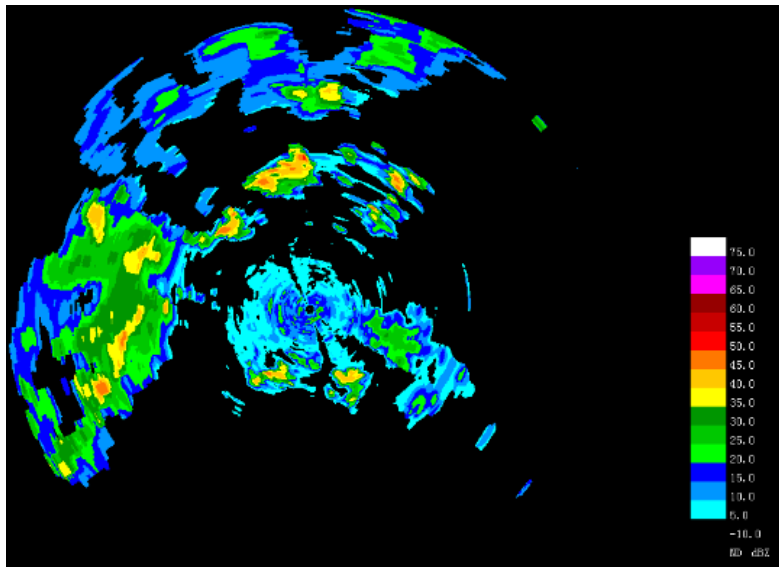
(a)

(b)

Figure 1 Raw Doppler weather radar mosaic as input (a) and processed radar mosaic as output (b)

Table 1 NWS standard reflectivity levels, and weather classification

NWS Level	Rainfall Rate a (mm/hr)	Reflectivity b (dBZ)	Color	Type
0	a<0.49	b<18	None	None
1	0.49≤a<2.7	18≤b<30	Light Green	Light Mist
2	2.7≤a<13.3	30≤b<41	Dark Green	Moderate
3	13.3≤a<27.3	41≤b<46	Yellow	Hazardous
4	27.3≤a<48.6	46≤b<50	Orange	Very Hazardous
5	48.6≤a<133.2	50≤b<57	Deep Orange	Intense
6	a≥133.2	b≥57	Red	Extreme

B. Fuel consumption and flight time

In this model, we only consider rerouting in horizontal plane. Because radar weather mosaic is published in 6-minute interval, we assume that each leg covers 6 minutes. Base of Aircraft Data (BADA) is used to calculate fuel consumption [23]. For the jet and turboprop engines, the thrust-specific fuel consumption, η (in kg/(min·kN)), is a function of the true airspeed, TAS (in knots), which is a scalar here.

$$\eta_i = C_{f1} \times \left(1 + \frac{TAS_i}{c_{f2}}\right) \tag{1}$$

where constants C_{f1} and C_{f2} are available from BADA and depend on the aircraft type. The nominal fuel flow, F (in kg/min), can then be calculated based on the thrust, Thr (in N), which also depends on the TAS implicitly:

$$F_i = \frac{\eta_i \times Thr}{1000} \tag{2}$$

Accordingly, the fuel consumption at altitude i is defined as (in kg):

$$\mathcal{F}_i = F_i \times T \times 60 \tag{3}$$

where T (in h) is the flying time obtained from Equation (4) without consider wind speed. Wind speed is a vector and L is flight distance (in km).

$$T = \frac{L}{1.852 \times TAS} \tag{4}$$

In order to illustrate the different fuel consumption in different flight altitude, we take aircraft A319 as an example. Figure 2 (*a*) shows that there is a decrease in fuel

consumption (unit in kg/min) from 7,500 to 11,900 meters, and an increase with TAS increasing. However, fuel consumption (unit in kg) at a given flight distance in 1000km will reach the minimum shown as the valley in Figure 2 (*b*), when TAS is adjusted to a special value.
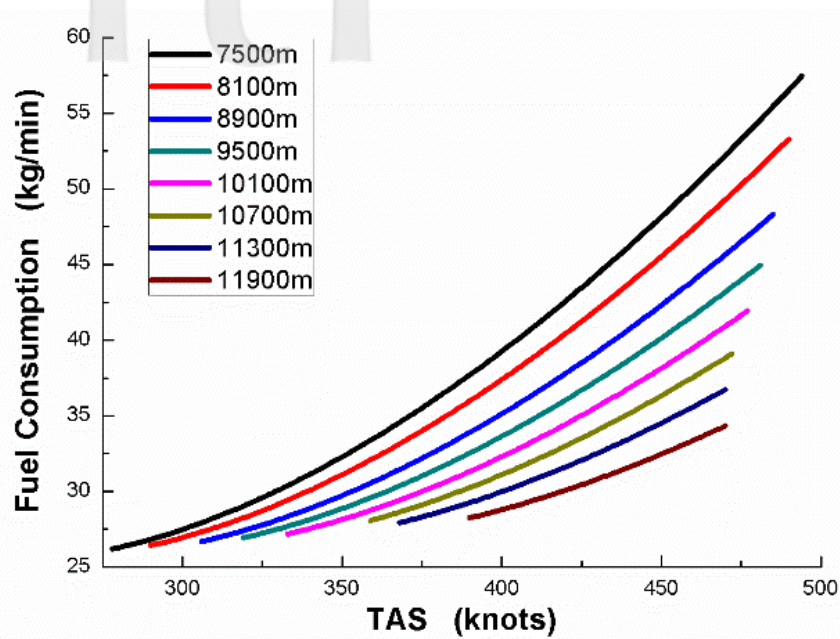
(*a*)
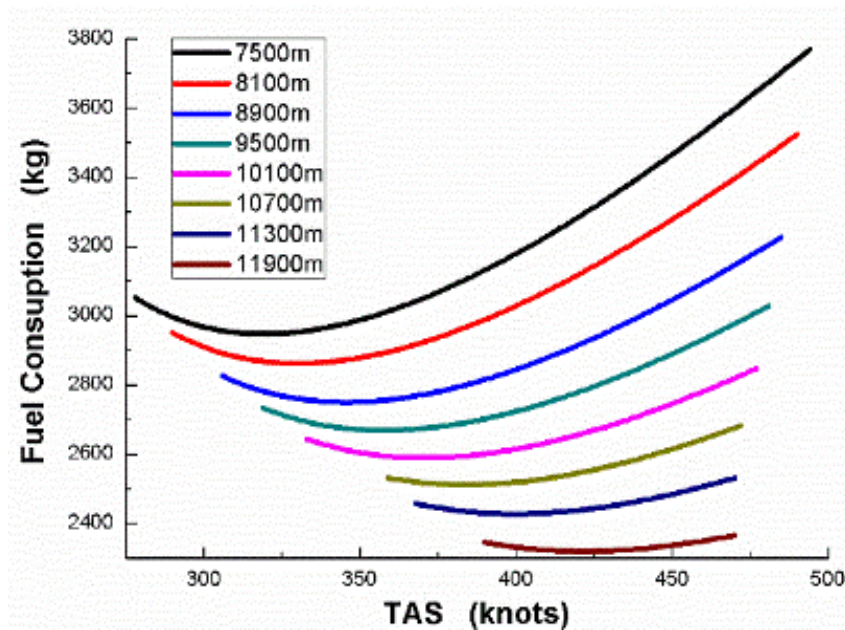
(*b*)

Figure 2 Fuel consumption in kg/min (*a*) and kg per 1000 km (*b*)

III. THE MULTI-OBJECTIVE OPTIMIZATION PROBLEM

It is a common practice for the ATC to change airplane time of departure to meet the requirement of different stakeholders such as airlines and passengers. In this section, we present the multi-objective optimization. The variables, objectives and constraints for the objective function will be described in details as follows.

A. Variables

The proposed optimization problem seeks the optimal decisions of time of departure in order to minimize fuel consumption, flight time and delay time. We outline the following variables and their definitions:

i:	Index of flight altitude
ATD:	Actual time of departure, decision variables
ETD	Estimated time of departure
DT:	Delay time caused by GDP
FT:	Flight time airborne
$\mathcal{F}C$:	Actual fuel consumption
L:	Rerouting path length
$\mathcal{F}uel^*$:	Planned fuel consumption
$Time^*$:	Planned flight time
MDT:	Maximum delay time caused by GDP

B.   Objective function

When the aircraft is detouring at altitude i, true airspeed (TAS) affects the flight time, and fuel consumption also relies on TAS and flight time. In our model, TAS is considered as a constant according to flight regulations from Filed Flight Plan Message (FPL). Therefore, the rerouting path length is a parameter that will affect the objective function:

$$\min \quad \alpha \times \frac{\mathcal{F}C}{\mathcal{F}uel^*} + \beta \times \frac{FT}{Time^*} + \gamma \times \frac{DT}{Time^*} \tag{5}$$

where $\mathcal{F}uel^*$ and $Time^*$ are planned fuel consumption and flight time from FPL, respectively. F^* is the nominal fuel flow in FPL altitude. In the above expression, we have that

$$FT = L/TAS \tag{6}$$

$$\mathcal{F}C_i = F_i \times FT \times 60 \tag{7}$$

$$\mathcal{F}uel^* = F^* \times Time^* \times 60 \tag{8}$$

$$DT = ADT - EDT \tag{9}$$

After simplifying the objective function, we have a new objective function shown as follows:

$$\min \quad \left(\alpha \times \frac{F_i}{F^*} + \beta\right) \times \frac{FT}{Time^*} + \gamma \times \frac{DT}{Time^*} \tag{10}$$

Because $Time^*$ is a constant, our objective function can be expressed as:

$$\min \quad \left(\alpha \times \frac{F_i}{F^*} + \beta\right) \times FT + \gamma \times DT \tag{11}$$

For simplification, we set $\delta = \alpha \times F_i/F^* + \beta$. The final objective function is expressed as weighted sum of flight time and delay time:

$$\min \quad \delta \times FT + \gamma \times D \tag{12}$$

C.   Constrains

We impose the constraints on the optimization problem as follows:

$$DT \leq MDT \tag{13}$$

$$\delta + \gamma = 1 \tag{14}$$

$$\delta, \gamma \in [0,1] \tag{15}$$

$$i \in \{1,2, \dots M\} \tag{16}$$

Constraint (13) stipulates that delay time must be less than or equal to maximum delay time. Otherwise, airlines would have to compensate passengers for long delay; (14)-(15) express the constraints for the weights; (15) specifies the feasible weight range, which is simply a non-negative constraint; (16) provides the set of feasible flight altitude indexes according to flight regulation.

D.   Algorithm

In order to meet the requirement of real-time rerouting, we have designed a novel real-time rerouting algorithm based on ant colony optimization (ACO). Real-time rerouting algorithm is illustrated in Figure 3. Firstly, if the planned route is influenced by severe weather, ACO is used to design the reroute path based on the severe weather area at time t. Then a new polygon is created by superposing severe weather at time t and $t + 1$. An encounter detection is necessary to judge whether flight route will penetrate severe weather cells. Note the flight route is only 6-minute-flight. If there is an encounter, we will design reroute path again based on the severe area at time t and $t + 1$. Then the airplane will fly for 6 minutes to a new point, which is a new starting rerouting point. This method is executed until airplane arrives at the destination, namely final rerouting point. At last, total reroute distance L can be obtained.
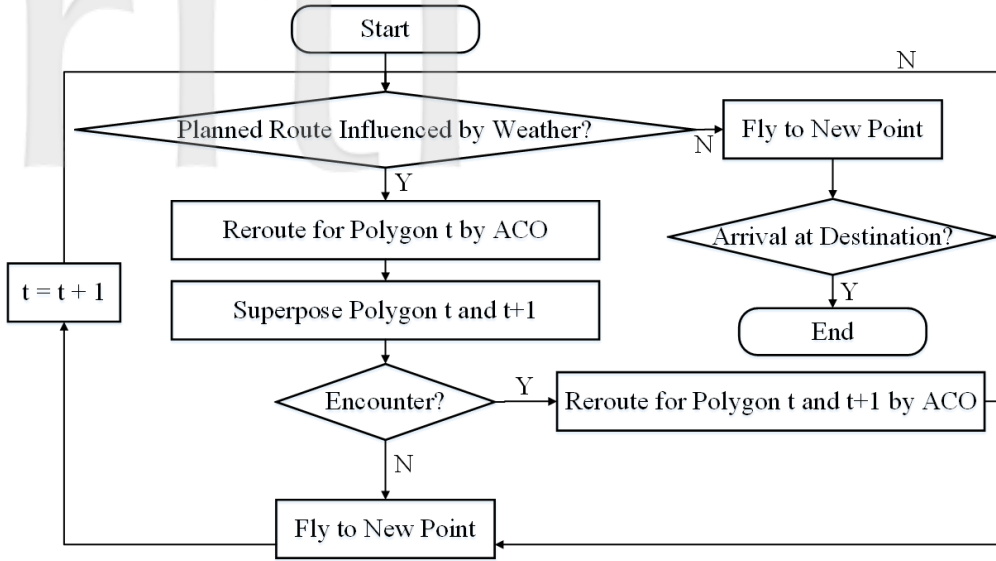
Figure 3 System architecture for dynamic reroute

The steps of ACO is explained as follows [24].

Step 1: Design a set of cells with 1 or 0 to represent the inaccessible and accessible areas of the airspace. In this paper, the grid numbered as 1 means that there is hazardous weather in this cell.

Step 2: Initialization of the pheromone matrix. Setting the starting point and destination point. In this step of calculation, we assume that pheromone for any location is equal.

Step 3: Select a node, which the ants are moving into the next step. Calculate the probability of heading to each node on the basic of pheromone in each node based on Equation (17). Finally, apply roulette algorithm for selecting next starting node.

$$p_{ij}^k = \begin{cases} \frac{[\tau_{ij}(t)]^a \times [\eta_{ij}]^b}{\sum_{k \in N(k)}[\tau_{ij}(t)]^a \times [\eta_{ij}]^b}, & j \in N(k) \\ 0, & others \end{cases} \qquad (17)$$

Note:

$\tau_{ij}(t)$:	pheromone density in arc (i,j)
η_{ij}:	heuristic information relevant to arc (i,j)
a ,b:	weight parameter of $\tau_{ij}(t)$ and η_{ij},respectively
$N(k)$:	feasible solution component set

Step 4: Update path and path length.

Step 5: Repeat Step 3 and 4 until ants arrive at destination point or there is no way to go.

Step 6: Repeat Step 3 to 5 until iterative process of m ants in some generation end.

Step 7: Update pheromone matrix. The ants are excluded in the calculation if they have not arrived at the destination. For the calculation details, please see Equation (18) and (19).

$$\tau_{ij}(t+1) = (1-\rho) \times \tau_{ij}(t) + \Delta\tau_{ij} \qquad (18)$$

$$\Delta\tau_{ij}(t) = \begin{cases} \frac{Q}{L_k(t)}, & ant\ k\ pass\ i,j \\ 0, & ant\ k\ does\ not\ pass\ i,j \end{cases} \qquad (19)$$

where $\rho \in (0,1]$ is pheromone evaporation parameter. Symbol Q is again a positive constant and $L_k(t)$ is the objective function value of the solution.

Step 8: Repeat Step 3 to 7 until iterative process of the n_{th} generation.

The values of each symbol adapted in Section IV are as follows: $a = 1; b = 7; \rho = 0.3; Q = 1$.

As the time of aircraft departure is discrete, we can get various delay time and flight time. As will be demonstrated, the model is a linear program and hence any Linear Programming (LP) solver can solve this problem.

IV. CASE STUDY

A. Reroute based on dynamic severe weather

As an example, we consider a flight path from ZHCC (Zhengzhou) to ZGGG (Guangzhou) with a distance of 1,070 km (from waypoint ZHO to waypoint P113) traveled by a B748 aircraft with a mass of 366,340 kg. TAS=900 km/h. Figure 4 shows the severe weather area and affected flight route. According to airlines regulations, the maximum delay time MDT is 30 minutes, if the delay time is more than 30 minutes, airlines have to pay the penalty. $\mathcal{F}uel^*$, $Time^*$ and flight altitude are 12,740 kg, 71 min and 9,800 m from FPL.

Figure 4 Severe weather area and affected flight routes

The radar mosaics are from 14:12 to 16:06 on April 09 2017. An example shown at 14:12 after the weather processing and hexagon envelop model processing is illustrated in Figure 5 (*a*).

After that, we place the flight forbidden area in the 54×54 grid-based background (see Figure 5 (*b*)), which are typically two dimensional grids with grid spacing of about 15km. We assume that the top left corner is the origin (0,0). The horizontal and vertical axes are x-axis and y-axis.

According to FPL, the flight should expected time over (*ETO*) ZHO at 14:12 and the estimated time of departure (*ETD*) is 13:57, because it takes 15 minutes for aircraft from Zhengzhou airport to ZHO. We assume that point ZHO is the starting reroute point, and P113 is the ending reroute point. Based on severe weather at 14:12, we use ACO to design rerouting path for the first 6-minute interval shown in Figure 6 (*a*). The aircraft flies 90 km in 6 minutes before next rerouting, on condition that TAS is a constant at 900 km/h. A circle is created with the S as its center and 90 kilometer distance as a radius. The intersection point of the ring and planed route is the next starting point for rerouting. We set this point as s_1. Using the method described in Figure 6, we can design the optimal reroute path step by step. To illustrate the iterations for a rerouting running, Figure 7 shows the trend of convergence curve. When the iteration reach 40, the optimal flight path and minimum flight path distance are obtained.
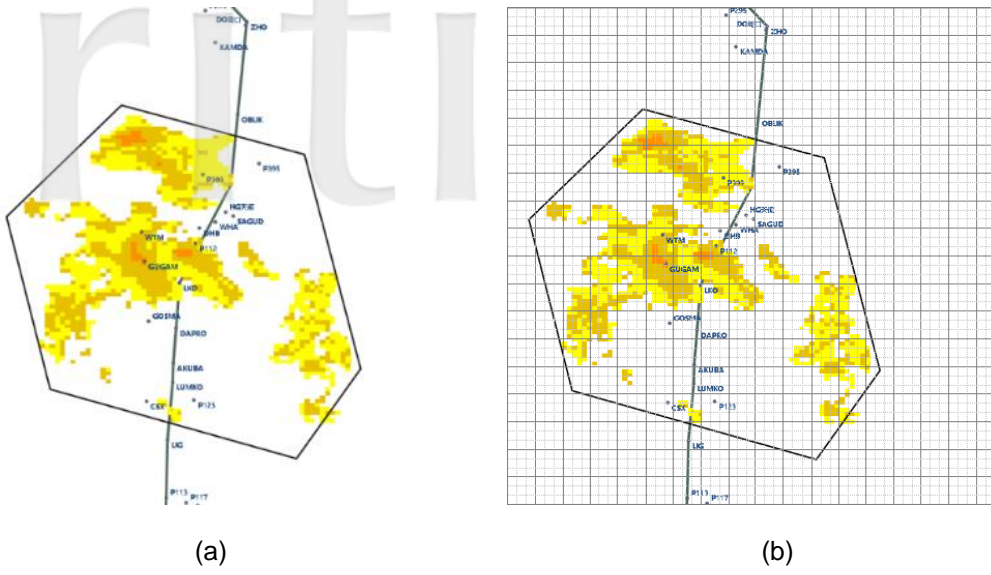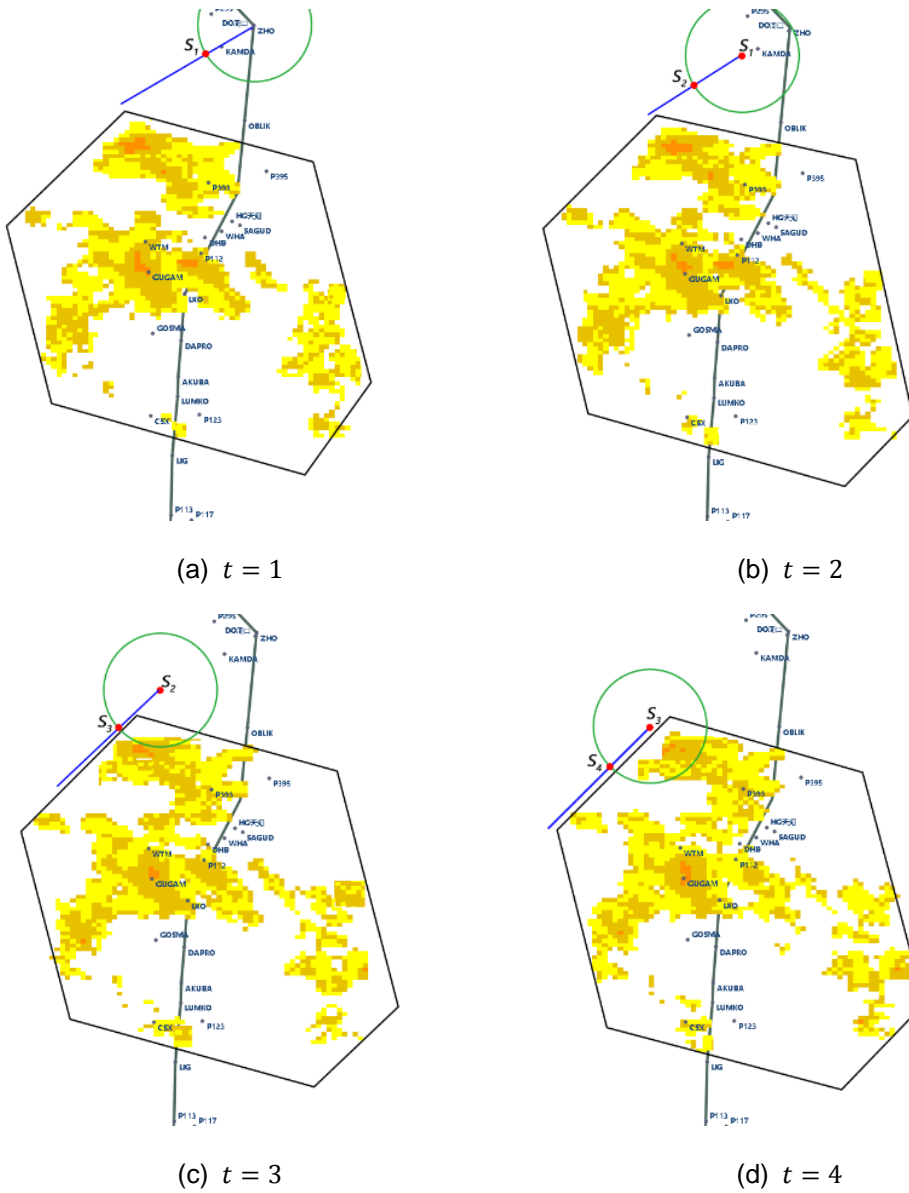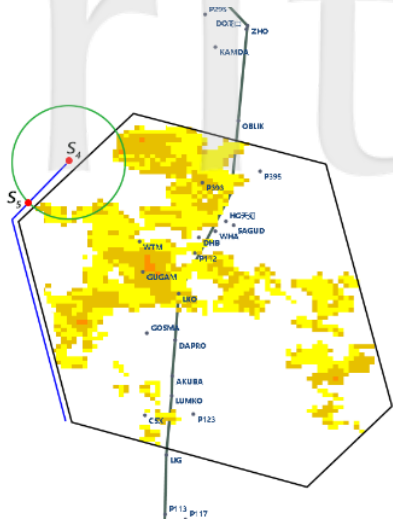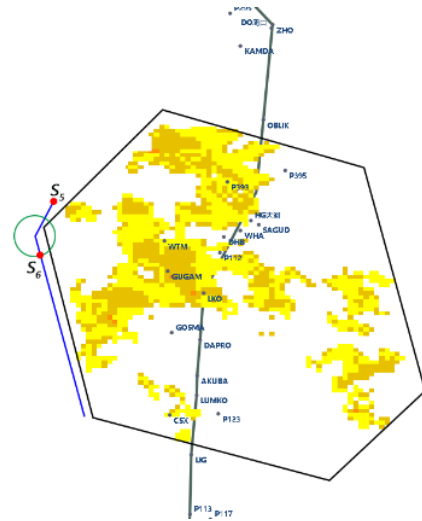
(a)

(b)

Figure 5 FFA at 14:12 flight path from ZHCC to ZGGG

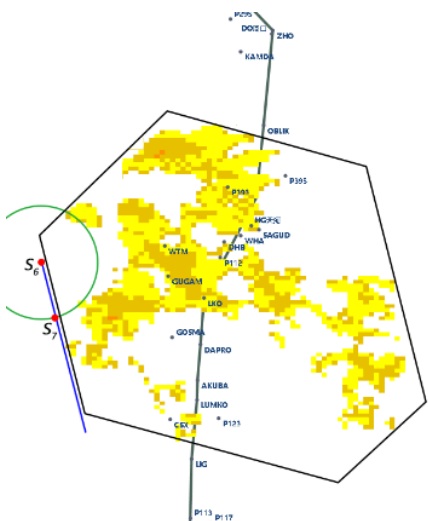

(a) $t = 1$

(b) $t = 2$

(c) $t = 3$

(d) $t = 4$

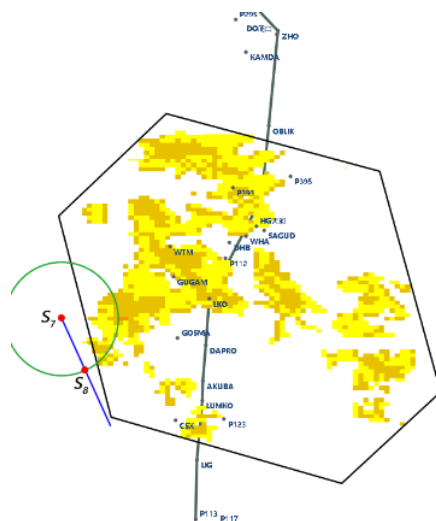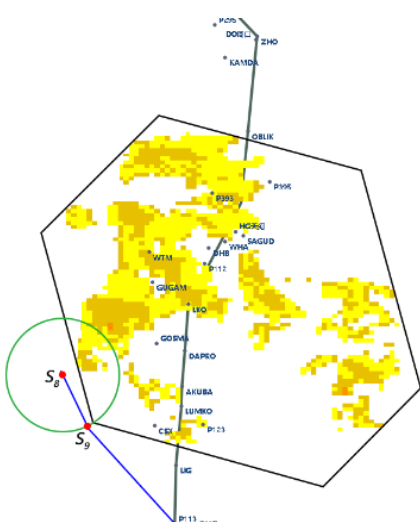(e) $t = 5$ (f) $t = 6$
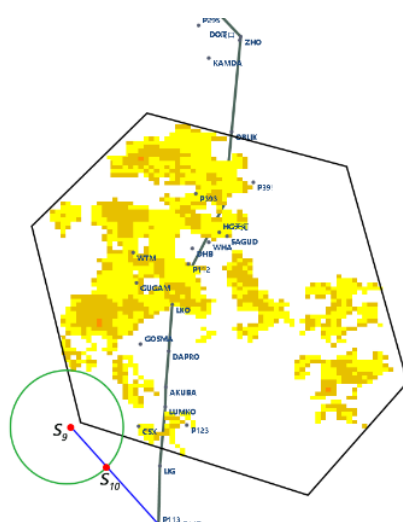
(g) $t = 7$ (h) $t = 8$

(i) $t = 9$ (j) $t = 10$
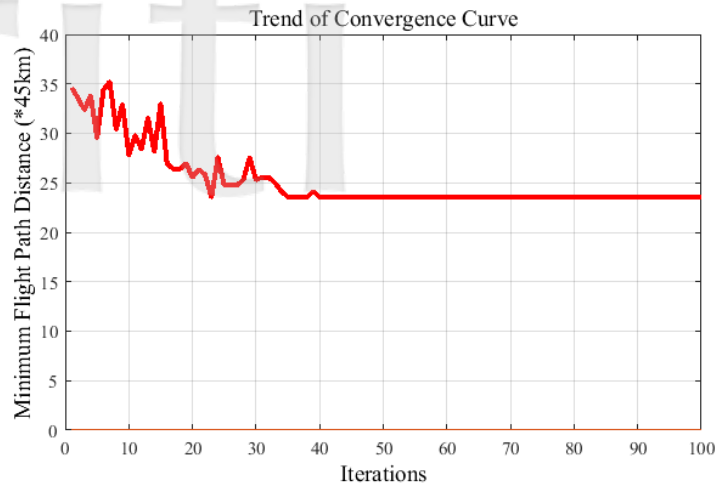
Figure 6 Reroute path from 14:12 to 15:06

Figure 7 Trend of convergence curve for a rerouting running.

B. Discussion

Table 2 has shown that there is a decrease in flight distance both in stationary reroute and dynamic reroute with the increase of DT generally. In this case study, optimal reroute path is on the west of FFA, and FFA is from west to east on the whole, but sometimes it dose move from east to west on a small scale, so there is a protrusion in Figure 8. Figure 8 shows the difference between stationary and dynamic reroutes obviously. Flight distance by dynamic reroute is approximately 6% shorter than that by stationary reroute. Note that this is an improvement that will save fuel consumption and reduce flight time.

Table 2 Comparison between stationary and dynamic reroutes

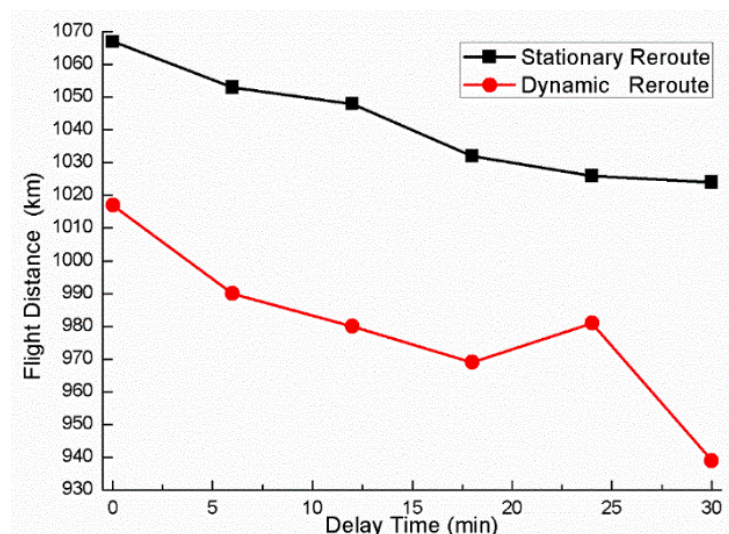| ATD	DT (min)	ETO	Stationary reroute (km)	Dynamic reroute (km)
13:57	0	14:12	1067	1017
14:03	6	14:18	1053	990
14:09	12	14:24	1048	980
14:15	18	14:30	1032	969
14:21	24	14:36	1026	981
14:27	30	14:42	1024	939

Figure 8 Comparison between stationary and dynamic reroutes at different delay time

C. Sensitivity Analysis

The sensitively analysis is to analyze how the output responses to the changes of the input variables [25]. In this section, we would make a discussion about the relationship between the delay time and flight time to find out the optimal time of departure for the designed algorithm. Delay time can be obtained by equation (9). When the airlines adopt different ATD, there are substantial differences in DT and FT (see Table 3). Nominal fuel flow can be calculated, and the result is $F = 178.6 \; kg/min$.

Table 3 Results in different time of departure

ATD	DT (min)	ETO	FT (min)	$\mathcal{FC}$ (kg)	L (km)
13:57	0	14:12	67.8	12,109	1,017
14:03	6	14:18	66	11,788	990
14:09	12	14:24	65.3	11,663	980
14:15	18	14:30	64.6	11,538	969
14:21	24	14:36	65.4	11,680	981
14:27	30	14:42	62.6	11,180	939

Table 4 has shown the trade-off between delay time and flight time in the optimal solution, as δ (flight time weight) changes from 0 to 1. The optimal time of departure for $\delta = 0, 0.1, \dots, 0.7$ is a constant 14:12. When $\delta = 0.8$, $\delta = 0.9$ and $\delta = 1$, the optimal time of departure are 14:18, 14:30 and 14:42, respectively. Figure 9 shows Pareto frontier about flight time and delay time.

Table 4 The trade-off between DT and FT in the optimal solution

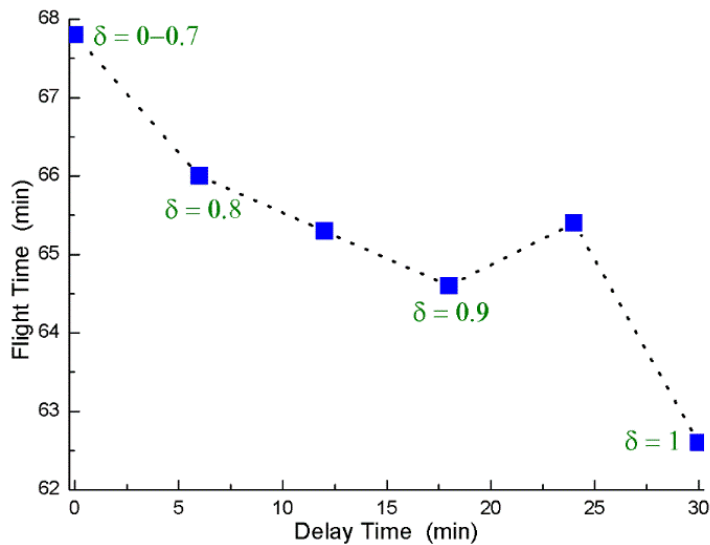| δ	DT (min)	FT (min)	ATD
0	0	67.8	13:57
0.1	0	67.8	13:57
0.2	0	67.8	13:57
0.3	0	67.8	13:57
0.4	0	67.8	13:57
0.5	0	67.8	13:57
0.6	0	67.8	13:57
0.7	0	67.8	13:57
0.8	6	66	14:03
0.9	18	64.6	14:15
1	30	62.6	14:27

Figure 9 Pareto frontier about delay time and flight time

V. CONCLUSIONS

This paper investigates the problem of choosing the optimal time of departure in the presence of severe weather. We propose a multi-objective optimization problem, considering weather-induced costs such as fuel consumption cost and time cost. The key parameters are delay time, flight time and fuel consumption. FFA can be obtained according to pilots' preference by filtering raw radar reflectivity data, which is the foundation for designing flight path to detour severe weather by ACO. Case study results show there is a decrease about 6% in flight distance by dynamic rerouting compared to stationary rerouting. When the aircraft is given different time of departure, delay time and flight time are various correspondingly. As the tradeoff δ varies, the optimal delay time and the flight time are shown in Pareto frontier. This method will provide a suitable decision on optimal time of departure for airlines and passengers.

ACKNOWLEDGMENTS

REFERENCES

[1] Hu MH, Xu XH, "Ground holding policy in air traffic flow control," *Journal of Nanjing University of Aeronautics & Astronautics*, Vol. 26, 1994, PP. 26–30.

[2] Agustı A, Alonso-Ayuso A, Escudero LF, Pizarro C, "On air traffic flow management with rerouting. Part II: Stochastic case," *European Journal of Operational Research*, Vol. 219, No. 1, 2012, pp. 167-177.

[3] Bertsimas D, Patterson SS, "The air traffic flow management problem with enroute capacities," *Operations research*, Vol. 46, No.3, 1998, pp. 406-422.

[4] Krozel J, Lee C, Mitchell JS, "Turn-constrained route planning for avoiding hazardous weather," *Air Traffic Control Quarterly,* Vol. 14, No.2, 2006, pp. 159-182.

[5] Mirosavljević P, Gvozdenović S, Čokorilo O, "The contribution of optimal turbo fan transport aircraft climb schedule to air company economy," *Technological and Economic Development of Economy*, Vol.15, No. 4, 2009, pp. 561-579.

[6] Liu JQ, Zhang ML, Chen PC, Xie JW, Zuo HF, "An integrative approach with sequential game to real-time gate assignment under CDM mechanism." Mathematical Problems in Engineering," 2014.

[7] Turgut ET, Usanmaz O, Ozan Canarslanlar A, Sahin O, "Energy and emission assessments of continuous descent approach," *Aircraft Engineering and Aerospace Technology*, Vol. 82, No. 1, 2010, pp. 32-38.

[8] Wilson I, Hafner F, "Benefit assessment of using continuous descent approaches at Atlanta," I*n 24th Digital Avionics Systems Conference*, *IEEE*, Vol. 1, 2005, pp. 2-B.

[9] Harada A, Ezaki T, Wakayama T, Oka K, "Air Traffic Efficiency Analysis of Airliner Scheduled Flights Using Collaborative Actions for Renovation of Air Traffic Systems Open Data," Journal of Advanced Transportation, 2018.

[10] McGovern A, Gagne DJ, Williams JK, Brown RA, Basara JB, "Enhancing understanding and improving prediction of severe weather through spatiotemporal relational learning," *Machine learning*, Vol. 95, No. 1, 2014, pp. 27-50.

[11] Wang F, Wang HY, "A re-routing path planning method based on Maklink graph and GA algorithm," *Journal of Transportation Systems Engineering and Information Technology*, Vol. 14, No. 5, 2014, pp. 154-160.

[12] Li X, Xu X, Dai F, Li D, "A new flight rerouting path planning algorithm and its applications," Chinese Control and Decision Conference. IEEE, 2009.

[13] Bertsimas D, Patterson SS, "The traffic flow management rerouting problem in air traffic control: A dynamic network flow approach," *Transportation Science*, Vol. 34, No. 3, 2000, pp. 239-255.

[14] Bokadia S, Valasek J, "Severe weather avoidance using informed heuristic search," AIAA Paper 4232, 2001.

[15] Krozel J, Penny S, Prete J, Mitchell JS, "Automated route generation for avoiding deterministic weather in transition airspace," *Journal of Guidance, Control, and Dynamics*, Vol. 30, No. 1, 2007, pp. 144-153.

[16] Ng HK, Grabbe S, Mukherjee A, "Design and evaluation of a dynamic programming flight routing algorithm using the convective weather avoidance model," AIAA guidance, navigation, and control conference. 2009.

[17] Sridhar B, Chatterji G, Grabbe S, Sheth K, "Integration of traffic flow management decisions," AIAA Guidance, Navigation, and Control Conference and Exhibit. 2002.

[18] Prete J, Mitchell J, "Safe routing of multiple aircraft flows in the presence of time-varying weather data," AIAA Guidance, Navigation, and Control Conference and Exhibit. 2004.

[19] Krozel J, Prete J, Mitchell JSB, Smith P, Andre AD, "Designing on-demand coded departure routes," AIAA Guidance, Navigation, and Control Conference and Exhibit. 2006.

[20] Han C, Liu Y, Ding X, Qiao J, Research and Improvement of Aircraft Rerouting Method Based on Flight Forbidden Areas. In 2016 3rd International Conference on Information Science and Control Engineering (ICISCE) (pp. 1044-1049). IEEE.

[21] Li X, "Flight rerouting path planning in severe weather," Nanjing. Nanjing University of Aeronautics and Astronautics 2009.

[22] Rhoda D, Kocab E, Pawlak M, "Aircraft Encounters with Thunderstorms in Enroute vs. Terminal Airspace above Memphis, Tennessee," 10th Conference on Aviation, Range, and Aerospace Meteorology. 2002.

[23] Nuic A, "User manual for the Base of Aircraft Data (BADA) revision 3.10," Atmosphere 2010 (2010): 001.

[24] Blum C, "Ant colony optimization: Introduction and recent trends," *Physics of Life reviews*, Vol. 2, No. 4, 2005, pp. 353-373.

[25] Saltelli A, Ratto M, Andres T, Campolongo F, Cariboni J, Gatelli D, Tarantola S, Global sensitivity analysis: the primer. John Wiley & Sons, 2008.